Journal of Hepatocellular Carcinoma

Dovepress
Taylor & Francis Group

Open Access Full Text Article

ORIGINAL RESEARCH

Prognostic Value of Clinical and CT Features in Camrelizumab Plus Apatinib Treatment for Unresectable Hepatocellular Carcinoma

Jinlian Che[1,2,*], Yidi Chen[2,*], Zhiming Zeng[3], Chenhui Li[2], Ling Zhang[2], Xialing Huang[2], Fuling Huang[2], Yingfei Wang[1], Weibao Huang[1], Bin Song[4,5], Liling Long[2]

[1]Department of Radiology, Maternal and Child Health Hospital of Guangxi Zhuang Autonomous Region, Nanning, Guangxi, People's Republic of China; [2]Department of Radiology, The First Affiliated Hospital of Guangxi Medical University, Nanning, Guangxi, People's Republic of China; [3]Department of Oncology, The First Affiliated Hospital of Guangxi Medical University, Nanning, Guangxi, People's Republic of China; [4]Department of Radiology, West China Hospital, Sichuan University, Chengdu, Sichuan, People's Republic of China; [5]Department of Radiology, Sanya People's Hospital, Sanya, Hainan, People's Republic of China

*These authors contributed equally to this work

Correspondence: Liling Long, Department of Radiology, The First Affiliated Hospital of Guangxi Medical University, No. 6 Shuangyong Road, Nanning, Guangxi, People's Republic of China, 530021, Tel +86 13807712604, Email cjr.longliling@vip.163.com

Background: Immunotherapy combined with targeted therapy is a key approach for patients with unresectable hepatocellular carcinoma (HCC). This study aimed to evaluate the prognostic value of clinical and CT features in Camrelizumab plus Apatinib treatment for these patients.

Materials and Methods: A retrospective study was conducted on unresectable HCC patients who received camrelizumab plus Apatinib treatment from June 2019 to August 2021. Clinical and contrast-enhanced CT features were analyzed. Logistic regression identified predictors of objective response, and Cox regression assessed prognostic factors for progression-free survival (PFS) and overall survival (OS). Nomograms were constructed based on independent predictors.

Results: Among 109 patients, the median OS was 20 months, median PFS was 9 months, and the ORR was 43.1%. Independent predictors of objective response included AFP ≥ 400 ng/mL (OR = 6.31), NLR ≥ 3.2 (OR = 3.72), tumor numbers ≥ 3 (OR = 3.93), and ΔAER < 15% (OR = 10.99), the AUC for objective response model was 0.874. Independent factors for PFS included AFP ≥ 400 ng/mL (HR = 2.04) and ΔAER < 15% (HR = 2.57), resulting in a model AUC of 0.859. Independent factors for OS were NLR ≥ 3.2 (HR = 2.07), Tumor numbers ≥ 3 (HR = 2.68), and extrahepatic metastasis (HR = 2.32), with an AUC of 0.848 and 0.866 for 1- and 2-year survival, respectively.

Conclusion: Clinical and contrast-enhanced show significant prognostic value in patients receiving Camrelizumab plus Apatinib. The developed models may assist in identifying responsive patients and personalizing treatment strategies.

Keywords: hepatocellular carcinoma, immunotherapy, targeted therapy, computerized tomography, objective response rate

Introduction

Hepatocellular carcinoma (HCC) ranks as the third leading cause of cancer-related deaths globally.[1] In China, it is the fourth most common malignancy and the second most fatal.[2] Despite advancements in screening protocols, approximately 70–80% of patients are diagnosed at intermediate to advanced stages, rendering them ineligible for surgical or localized curative treatments.[3]

Targeted therapy and immunotherapy are now the standard of care for these patients.[4] Targeted therapies work by directly inhibiting tumor growth and blocking angiogenesis, thereby restricting tumor vascularization. Immunotherapy, particularly immune checkpoint inhibitors, reactivates immune cells by overcoming immune tolerance, restoring tumor-specific immunity.[5] Studies have shown that combining targeted therapy with immunotherapy can have a synergistic

Received: 11 March 2025
Accepted: 6 September 2025
Published: 9 October 2025

effect, suppressing tumor cell proliferation, inhibiting angiogenesis, and ultimately leading to tumor necrosis and an immune response.[6] Since anti-angiogenic therapies targeting VEGF ligands can mitigate the local immunosuppressive effects of VEGF signaling and promote T cell infiltration, numerous clinical trials have demonstrated promising outcomes.[7] IMbrave150 and CARES-310 have shown that combining PD-1/PD-L1 inhibitors with anti-angiogenic agents enhances immunogenicity and clinical outcomes in unresectable HCC.[8]

Although immunotherapy and targeted therapy have emerged as standard options, identifying appropriate candidates remains a challenge, the objective response rate, overall survival (OS) and progression-free survival (PFS) outcomes have not met expectations.[8] Additionally, these therapies come with significant side effects; immune-related adverse events occur in 66% of cases, with grade 3 or higher adverse reactions in approximately 14%.[9] Therefore, identifying patients likely to benefit from these therapies is crucial, allowing clinicians to avoid ineffective or excessive treatment. Previous studies[10–12] suggest that clinical features (eg, AFP, prothrombin induced by vitamin K absence-II [PIVKA-II], NLR, PLR, HBV-DNA), and imaging characteristics (eg, tumor size, multifocality, vascular invasion, tumor margin, capsule, arterial enhancement) are important prognostic factors. Combining these features may help non-invasively and accurately predict treatment outcomes before therapy.

Camrelizumab combined with Apatinib is a widely used immunotherapy and targeted therapy regimen for HCC.[13,14] While there is currently no consensus regarding reliable imaging biomarkers to guide optimal patient selection. In clinical practice, the treatment plan for patients is usually determined through multidisciplinary team. CT-based prognostic models have been proposed to evaluate microvascular invasion,[15] and intratumoral characteristics (eg identifying proliferative HCC) in HCC treated with transarterial chemoembolization.[12] The decrease ratio of arterial enhancement (ΔAER) reflects the anti-angiogenic impact of treatment and may serve as an early surrogate marker of tumor ischemia. Colagrande et al[16] demonstrated that CT-derived enhancement volume changes predicted response to sorafenib.

To date, no studies have validated ΔAER in the Camrelizumab-Apatinib setting, as well as limited CT-drived models exist for Camrelizumab-Apatinib therapy. Meanwhile, international guidelines increasingly favor atezolizumab–bevacizumab based on IMbrave150 trial outcomes, which demonstrated superior overall survival compared to sorafenib. Nonetheless, due to drug accessibility, toxicity profile, and patient-specific factors, Camrelizumab-Apatinib remains widely used in China.[6]

This study aims to evaluate the association between baseline clinical characteristics and CT imaging features with treatment outcomes, including objective response, PFS and OS. Furthermore, we seek to identify independent prognostic factors for long-term survival and to develop a predictive model to facilitate individualized treatment strategies and prognostic assessment.

Materials and Methods

Conflict of Interest and Ethical Approval

This study was approved by the Ethics Committee of our institution (Approval No: 2023-K012-01) and conducted in accordance with the Declaration of Helsinki. The authors declare no conflicts of interest, financial or otherwise, related to this study. As this was a retrospective study based on anonymized data, the Ethics Committee waived the requirement for informed consent. All patient data were de-identified, and strict confidentiality was maintained throughout the study in compliance with institutional and national data protection regulations.

Study Design and Patient Selection

This retrospective study included 109 patients who were diagnosed with HCC and received combined immunotherapy and targeted therapy (Camrelizumab and Apatinib) at our hospital between June 2019 and August 2021. The inclusion criteria were as follows: (1) diagnosis of HCC based on based on criteria as defined by the AASLD guidelines; (2) deemed unsuitable for surgery or local treatment by a multidisciplinary team; (3) completed clinical records; (4) pre-treatment enhanced CT performed within two weeks of therapy initiation; (5) at least one measurable intrahepatic lesion (tumor size ≥ 10 mm). Exclusion criteria included: (1) receipt of other HCC-specific treatments prior to the therapy (eg radiotherapy, transarterial radioembolization, transhepatic arterial chemotherapy and embolization), according to this

study protocol, patients may receive additional treatments following disease progression; (2) follow-up period less than two months; (3) no follow-up enhanced CT assessment during the study period; (4) post-resection patients with no measurable intrahepatic lesions receiving adjuvant therapy; (5) poor image quality that precluded assessment.

Data Collection

Patient clinical data included age, sex, hepatitis, cirrhosis, smoking and alcohol use, liver fluke infection, family history of liver disease, hypertension, and diabetes. Additionally, Barcelona Clinic Liver Cancer (BCLC) staging, Child-Pugh liver function classification, and Eastern Cooperative Oncology Group (ECOG) performance status were recorded. Peripheral blood samples were collected within one week before therapy initiation to measure neutrophil, lymphocyte, and platelet counts, serum alpha-fetoprotein (AFP), prothrombin induced by vitamin K absence-II (PIVKA-II), albumin (ALB), alanine aminotransferase (ALT), aspartate aminotransferase (AST), and hepatitis B virus DNA (HBV-DNA) levels.

Treatment Protocol and Follow-Up

All patients were treated with Camrelizumab 200 mg on day 1 (intravenous infusion every two weeks) and Apatinib 250 mg (oral, once daily). Dose adjustments or discontinuation were made by the attending physician based on adverse events or disease progression. Patients were followed up every 6–8 weeks, with each visit including clinical interviews, physical examinations, routine blood tests, liver function tests, AFP, PIVKA-II, and HBV-DNA levels. Imaging follow-up primarily included multi-phase enhanced CT, MRI, contrast-enhanced ultrasound, or PET-CT. The cut-off date for follow-up was January 31, 2023.

The Primary endpoints were objective response rate (ORR) and progression-free survival (PFS), ORR referring to the proportion of patients whose tumor size has decreased to a pre-defined value and can be maintained for the minimum required time limit (4 weeks), which includes both complete responses (CR) and partial responses (PR), with ORR = CR + PR. PFS was defined as the time from the start of treatment to disease progression or death, whichever occurred first. Secondary endpoint was overall survival (OS), OS was defined as the time from the start of treatment to death from any cause or the last known follow-up.

CT Scanning Equipment and Protocol

CT scans were performed using 256-slice spiral CT (Revolution, GE), or dual-energy CT (SOMATOM Definition Flash or Force CT, Siemens). Detailed protocols are provided in Supplemental Table S1.

CT Image Analysis

Two radiologists (C.JL and C.YD) with over 10 years of experience in diagnosing abdominal diseases independently reviewed the enhanced CT images, without knowledge of the patients' clinical information. The analyzed features included tumor size, tumor numbers, tumor margin, internal artery, peritumoral contrast enhancement, tumor in vein and the decrease ratio of arterial phase contrast-enhancement (ΔAER). AER = [(HUpost−HUpre)/HUpre]×100%. HU was measured from the same ROI on arterial phase image (HUpost) and non-contrast enhancement image (HUpre). ΔAER = AER_untreated−AER_post-treated. In cases of disagreement between the two radiologists, a third radiologist (L.LL) with over 25 years of experience in liver disease diagnosis was consulted to reach a consensus. Interobserver agreement between the two radiologists was assessed using Cohen's kappa, agreement was good to excellent for all evaluated features (kappa: 0.72–0.86). Detailed definitions of the evaluated CT imaging features and those interobserver agreement are provided in Supplemental Table S2.

Statistical Analysis

All statistical analyses were performed using SPSS version 25.0 (IBM, Chicago, USA) and R version 4.1.2 (http://www.r-project.org/). The Shapiro–Wilk test was used to assess the normality of continuous variables. Normally distributed data were expressed as mean ± standard deviation, while non-normally distributed data were expressed as median and interquartile range. Independent samples t-tests were used to compare normally distributed data between groups, while

the Mann–Whitney *U*-test was used for non-normally distributed data. Continuous variables were converted to categorical variables where appropriate based on clinical or reference cut-off values. Categorical variables were expressed as frequencies and percentages, with comparisons made using the chi-square test or Fisher's exact test as needed. Logistic regression was used to identify independent factors for the OR.

Survival curves for PFS and OS were generated using the Kaplan-Meier method, and differences between groups were compared using the Log rank test. Univariate Cox proportional hazard models were used to identify potential factors influencing treatment efficacy and survival, and variables with $P < 0.05$ were included in multivariate Cox analysis to determine independent prognostic factors. These factors were incorporated into a predictive model, and a nomogram was constructed. The model's accuracy and utility were evaluated using the concordance index (C-index), receiver operating characteristic (ROC) curves, calibration curves, and decision curve analysis (DCA). Interobserver agreement was assessed using the kappa statistic, with $P < 0.05$ considered statistically significant.

Results

Patient Characteristics

A total of 209 patients were initially considered for this study. After applying the exclusion criteria, 100 patients were excluded for various reasons: 42 had received other HCC specific treatments within the previous three months, 16 had follow-up durations of less than two months, 22 lacked follow-up enhanced CT imaging, and 20 had no measurable intrahepatic lesions (multiple lesions, but the size of each lesion is less than 10 mm). Therefore, 109 patients were included in the final analysis (Figure 1).

The median age of the cohort was 48.87±11.5 years (range: 25–76). Of the 109 patients, 95 were male, and 14 were female. The majority of patients (102) had a history of hepatitis B, 3 had hepatitis C, and 12 had a history of liver fluke infection. Additionally, 95 had clinically diagnosed cirrhosis, 12 had hypertension, and 14 had diabetes. Regarding functional status, 74 patients had an ECOG performance status (PS) of 0, while 35 had a PS of 1. Child-Pugh liver function classifications were A in 98 patients and B in 11. In terms of cancer staging, 84 patients were classified as BCLC stage B, and 25 were at stage C. The median value of neutrophil count was 4.13×10^9/L (range: 2.79–5.43 $\times10^9$/L), platelet count was194.00×10^9/L (range: 145.85–242.00 $\times10^9$/L), lymphocyte count was1.21×10^9/L (range: 1.01–1.62 $\times10^9$/L). Serum AFP levels were recorded with a median value of 446.16 ng/mL (range: 40.33–18,459.42), and PIVKA-II levels had a median of 2320.38 mAU/mL (range: 278.64–19,227.86). The detailed demographic and clinical characteristics are presented in Table 1.

The median tumor size was 10.05 cm (range: 6.88–13.87 cm). A total of 52 patients had extrahepatic metastases, with 34 cases involving the lungs, 31 in the abdominal cavity, and 1 case of bone metastasis. Vascular invasion was seen in 60 patients with portal vein involvement, 25 with hepatic vein involvement, and 8 with inferior vena cava involvement. Single tumors were present in 30.3% (33/109) of patients, while 69.7% (76/109) had multi-tumors.

Patients Follow-Up

During the follow-up period, 54 patients died, 20 were lost to follow-up, and 35 remained alive. The median overall survival (mOS) was 20 months (95% CI: 15.47–24.52), with a median follow-up time of 22 months (95% CI: 17.9–26.1). The median PFS was 9 months (95% CI: 7.0–11.0). The ORR was 43.1%, and the disease control rate (DCR) was 75.2%. Based on mRECIST criteria, treatment responses included complete response (CR) in 13 patients, partial response (PR) in 34 patients, stable disease (SD) in 35 patients, and progressive disease (PD) in 27 patients. The ORR was calculated by combining CR and PR, totaling 43.1% (47/109), while SD and PD were classified as non-responders.

Predictive Value of Clinical and CT Features for Treatment Efficacy (OR)

The clinical and CT features of patients in the objective response group (OR group) were compared with those of the non-responders group (non-OR) in Supplemental Tables S3 and S4, respectively. Multivariate analysis identified four independent risk factors associated with treatment response: AFP ≥ 400 ng/mL (OR = 6.31, p = 0.001), neutrophil-to-lymphocyte ratio (NLR) ≥ 3.2 (OR = 3.72, p = 0.012), tumor numbers ≥ 3 (OR = 3.93, p = 0.011), and a decrease ratio of arterial phase

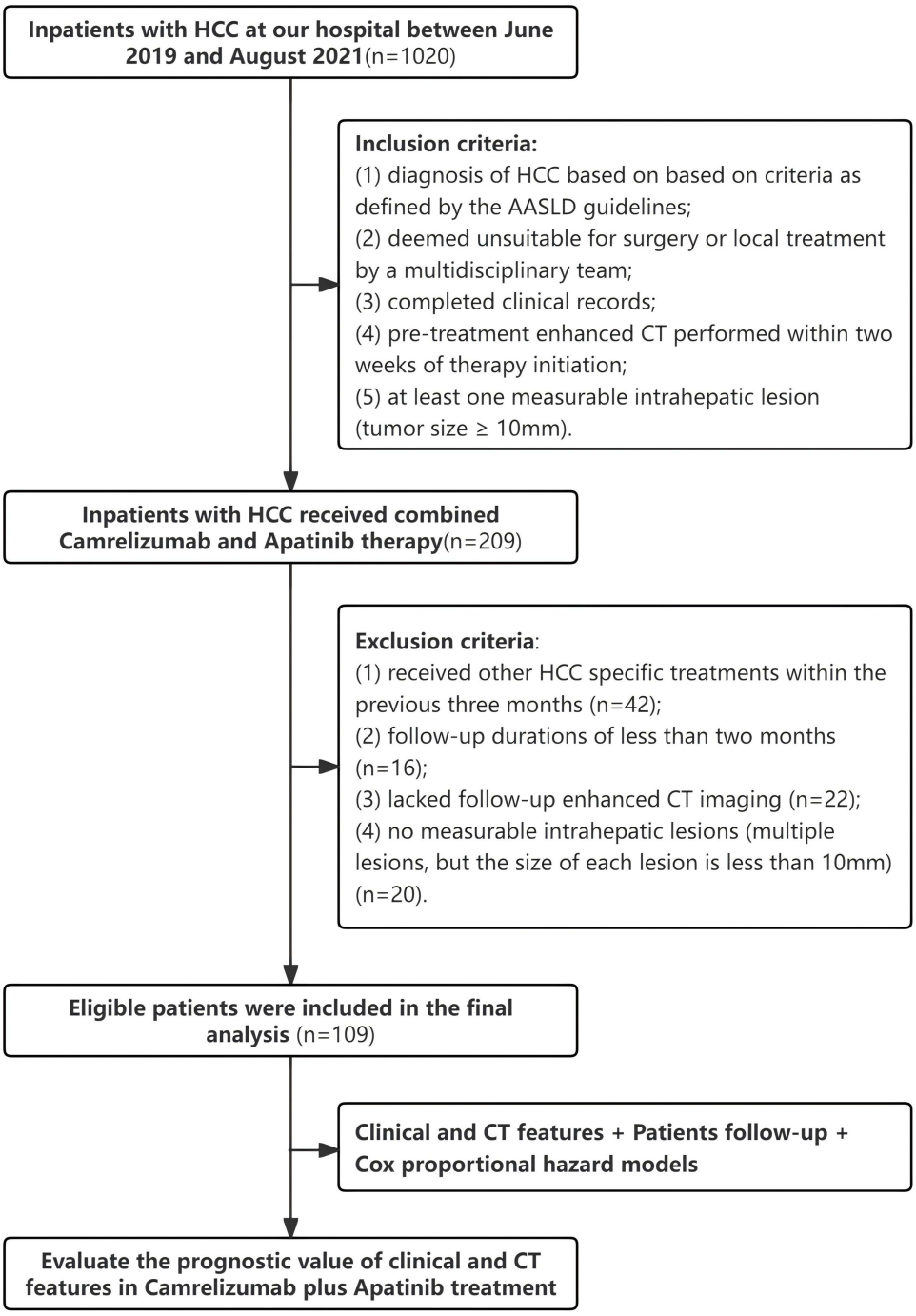

Figure 1 The flow diagram of the study cohort. A total of 109 participants were included in this study.

contrast-enhancement (ΔAER) < 15% (OR = 10.99, p < 0.001) (Table 2). These variables were incorporated into a predictive model for ORR. The model's area under the curve (AUC) was 0.874 (95% CI: 0.804–0.941) (Figure 2). Nomogram was built based on the clinical and CT features to predict the therapeutic response, the calibration curve demonstrated good agreement between the predicted and observed outcomes, and the DCA confirmed the clinical benefit of the model (Figure 3).

Table 1 The Detailed Demographic and Clinical Characteristics of This Study Cohort

Characteristics	All (n = 109)	OR (n = 47)	Non-OR (n = 62)	*P* value
Age (years)	48.87±11.5	50.00±10.57	48.02±12.28	0.378
Gender				0.239
Male	87.2% (95/109)	45.3% (43/95)	54.7% (52/95)	
Female	12.8% (14/109)	28.6% (4/14)	71.4% (10/14)	
Hepatitis B				0.683
Absence	6.4% (7/109)	28.6% (2/7)	71.4% (5/7)	
Presence	93.6% (102/109)	44.1% (45/102)	55.9% (57/102)	
Cirrhosis				0.578
Absence	12.8% (14/109)	50.0% (7/14)	50.0% (7/14)	
Presence	87.2% (95/109)	42.1% (40/95)	57.9% (55/95)	
Hypertension				0.610
Absence	88.9% (97/109)	42.3% (41/97)	57.7% (56/97)	
Presence	11.1% (12/109)	50.0% (6/12)	50.0% (6/12)	
Diabetes				0.256
Absence	87.2% (95/109)	41.1% (39/95)	58.9% (56/95)	
Presence	12.8% (14/109)	57.1% (8/14)	42.9% (6/14)	
BCLC stage				0.307
B	22.9% (25/109)	52.0% (13/25)	48.0% (12/25)	
C	77.1% (84/109)	40.5% (34/84)	59.5% (50/84)	
Child-pug				0.633
A	10.1% (98/109)	43.9% (43/98)	56.1% (55/98)	
B	89.9% (11/109)	36.4% (4/11)	63.6% (7/11)	
ECOG PS				0.102
0	67.8% (74/109)	48.6% (36/74)	51.4% (38/74)	
1	32.2% (35/109)	31.4% (11/35)	68.6% (24/35)	
AFP				<0.001
<400 ng/mL	48.6% (53/109)	62.3% (33/53)	33.7% (20/53)	
≧400 ng/mL	51.4% (56/109)	25.0% (14/56)	75.0% (42/56)	
PIVKA-II				0.003
<732 mAU/mL	41.3% (45/109)	60.0% (27/45)	40.0% (18/45)	
≧732 mAU/mL	58.7% (64/109)	31.3% (20/64)	68.7% (44/64)	
Albumin g/L	34.79±4.56	34.22±4.54	35.22±4.57	0.258
ALT				0.067
<38.5 U/L	56.0% (61/109)	50.8% (31/61)	49.2% (30/61)	
≧38.5 U/L	44.0% (48/109)	33.3% (16/48)	66.7% (32/48)	
AST				0.014
<63.5 U/L	56.9% (62/109)	53.2% (33/62)	46.8% (29/62)	
≧63.5 U/L	43.1% (47/109)	29.8% (14/47)	70.2% (33/47)	
NLR				<0.001
<3.2	51.4% (56/109)	60.7% (34/56)	39.3% (22/56)	
≧3.2	48.6% (53/109)	24.5% (13/53)	75.5% (40/53)	
PLR				0.012
<136.2	45.9% (50/109)	56.0% (28/50)	44.0% (22/50)	
≧136.2	54.1% (59/109)	32.2% (19/59)	67.8% (40/59)	
HBV-DNA				0.921
$<10^4$ (IU/ mL)	63.3% (69/109)	43.5% (30/69)	56.5% (39/60)	
≧10^4 (IU/ mL)	36.7% (40/109)	42.5% (17/40)	57.5% (23/40)	

Abbreviations: OR, objective response; AFP, alpha-fetoprotein; PIVKA-II, prothrombin induced by vitamin K absence-II; ALT, alanine aminotransferase; AST, aspartate aminotransferase; NLR, neutrophil-to-lymphocyte ratio; PLR, platelet-to-lymphocyte ratio; HBV-DNA, Hepatitis B virus DNA load; BCLC stage, Barcelona clinic liver cancer staging system; ECOG PS, eastern cooperative oncology group performance status.

Table 2 Multivariate Logistic Regression Analysis of Clinical and CT Features for Objective Response

Variable	β	*P* values	OR	95% CI
AFP (≥400 vs <400 ng/mL)	1.84	0.001	6.31	2.19–18.19
PIVKA-II (≥732 vs <732 mAU/mL)	0.76	0.185	2.14	0.69–6.58
NLR (≥3.2 vs <3.2)	1.31	0.012	3.72	1.34–10.34
PLR (≥136.2 vs <136.2)	0.31	0.611	1.36	0.42–4.43
AST (≥63.5 vs <63.5 U/L)	0.59	0.296	1.80	0.59–5.46
Tumor numbers (≥3 vs <3)	1.37	0.011	3.93	1.37–11.29
Peritumoral contrast enhancement (Presence vs Absence)	0.71	0.193	2.03	0.70–5.86
Extrahepatic metastases (Presence vs Absence)	0.61	0.275	1.84	0.62–5.51
ΔAER (<15% vs ≥15%)	2.39	<0.001	10.99	3.53–34.19

Abbreviations: ORR, Objective response rate; β, regression coefficient; OR, odds ratio; AFP, alpha-fetoprotein; PIVKA-II, prothrombin induced by vitamin K absence-II; AST, aspartate aminotransferase; NLR, neutrophil-to-lymphocyte ratio; PLR, platelet-to-lymphocyte ratio; ΔAER, decrease ratio of arterial phase contrast-enhancement.

Predictive Value of Clinical and CT Features for PFS

Univariate and Multivariate Cox Regression Analysis for PFS

Independent factors predicting progression-free survival included AFP ≥ 400 ng/mL (HR = 2.04, 95% CI: 1.15–3.64, p = 0.015), PIVKA-II ≥ 732 mAU/mL (HR = 2.05, 95% CI: 1.14–3.66, p = 0.016), tumor numbers ≥ 3 (HR = 2.53, 95% CI: 1.47–4.34, p = 0.001), and ΔAER < 15% (HR = 2.57, 95% CI: 1.54–4.33, p < 0.001). Detailed results are presented in Table 3.

PFS Predictive Model Construction and Validation

The PFS predictive model was constructed using the significant variables (AFP, PIVKA-II, tumor numbers, and ΔAER), yielding an AUC of 0.859 (95% CI: 0.803–0.959). The AUC was notably higher than that of BCLC stage alone (0.578, 95% CI 0.468–0.688). Nomogram was built based on the clinical and CT features to predict the PFS, the calibration curve showed good overlap with the reference line, and the DCA supported the model's value in clinical decision-making (Figure 4).

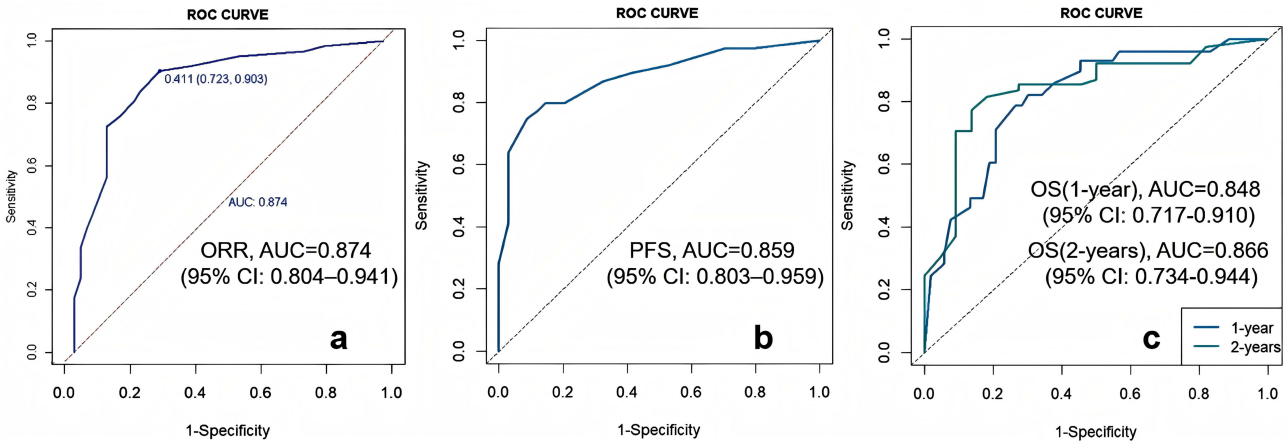

Figure 2 Receiver operating characteristic (ROC) curve of clinical and CT features (prediction models) for objective response (**a**), progression-free survival (**b**) and overall survival (**c**); (**a**) the area under receiver operating characteristic curve (AUC) of prediction model for objective response was 0.874, 95% confidence interval (CI) was 0.804–0.941; (**b**) the AUC of prediction model for progression-free survival was 0.859 (95% CI: 0.803–0.959); (**c**) the AUC of prediction model for 1-year and 2-years overall survival was 0.848 (95% CI: 0.717–0.910) and 0.866 (95% CI: 0.734–0.944), respectively.

https://doi.org/10.2147/JHC.S527624

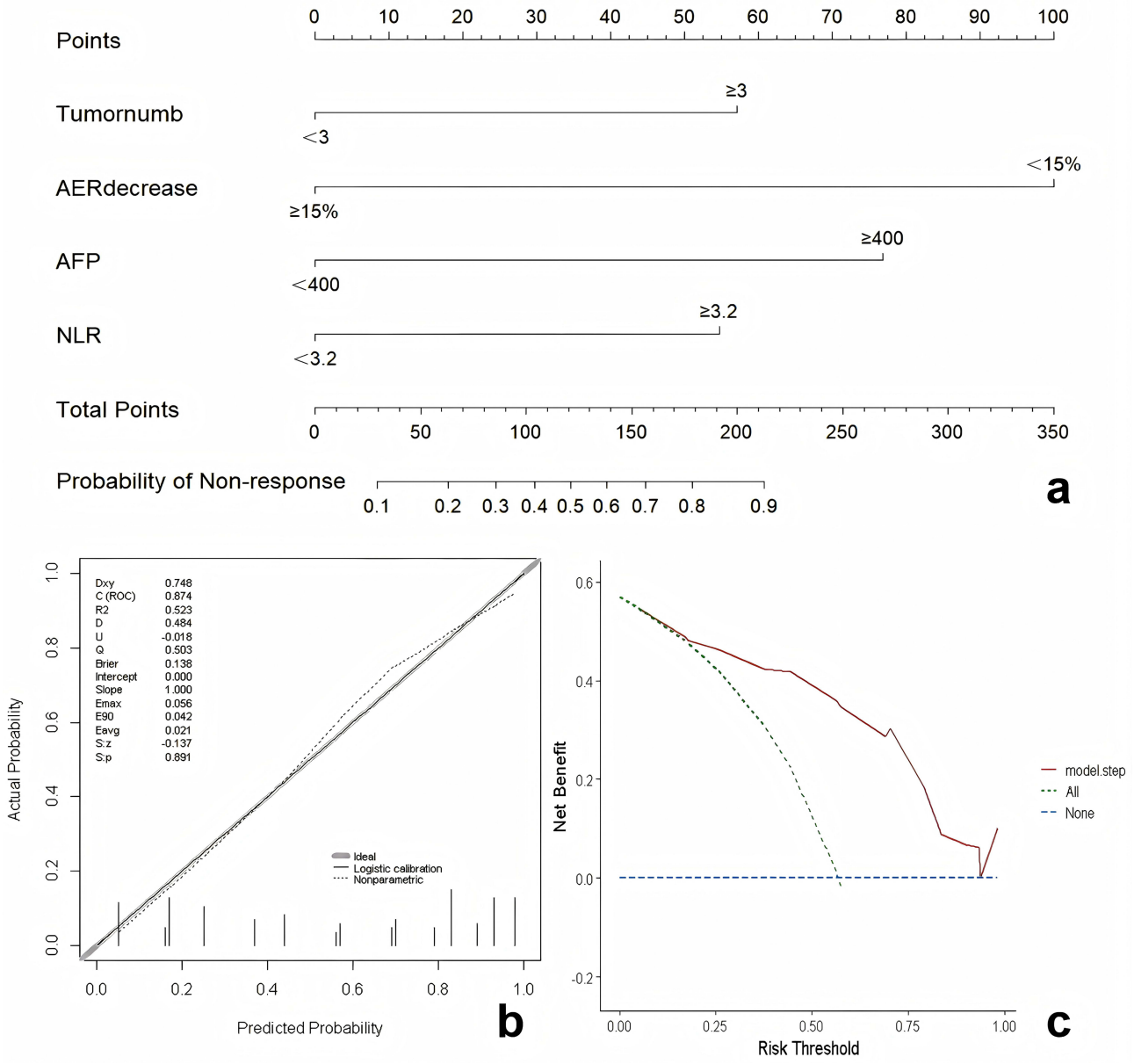

Figure 3 The nomogram to predict objective response in Camrelizumab plus Apatinib treatment for unresectable hepatocellular carcinoma. (**a**) The nomogram was developed with alpha-fetoprotein (AFP), neutrophil-to-lymphocyte ratio (NLR), tumor numbers, and a decrease ratio of arterial phase contrast-enhancement (ΔAER). A vertical line was made according to the value of the total points to determine the probability of objective response. (**b**) Validity of the predictive performance of the nomogram in estimating the risk of objective response in the 1,000 bootstrap resamples. (**c**) Decision curve analysis (DCA) of the prediction model, the x-axis shows the probability threshold that is the minimum predicted risk at which treatment would be chosen. The y-axis shows net benefit, interpreted as the number of true-positive decisions per patient after accounting for unnecessary treatments. Model curves are compared with treat-all and treat-none; higher net benefit indicates greater clinical utility.

Predictive Value of Clinical and CT Features for OS

Univariate and Multivariate Cox Regression Analysis for OS

Several factors were identified as independent predictors of overall survival through Cox regression analysis. These included NLR ≥ 3.2 (HR = 2.07, 95% CI: 1.15–3.73, p = 0.015), tumor numbers ≥ 3 (HR = 2.68, 95% CI: 1.38–5.21, p = 0.004), peritumoral enhancement (present vs absent, HR = 1.81, 95% CI: 0.98–3.33, p = 0.05), presence of extrahepatic metastasis (HR = 2.32, 95% CI: 1.21–4.44, p = 0.011), and ΔAER < 15% (HR = 2.16, 95% CI: 1.22–3.83, p = 0.009). Detailed results are provided in Table 4.

Table 3 Univariate and Multivariate Cox Regression Analysis of Clinical and CT Features for Progression-Free Survival

Variable	Univariate Cox Regression		Multivariate Cox Regression	
	HR (95% CI)	*P* value	HR (95% CI)	*P* value
Age (≥60 vs <60years)	1.32(0.71–2.45)	0.375	—	
Gender (male vs female)	1.06(0.54–2.08)	0.870	—	
Hepatitis B (Presence vs Absence)	1.86(0.45–7.64)	0.387	—	
Cirrhosis (Presence vs Absence)	1.25(0.59–2.63)	0.553	—	
BCLC stage (C vs B)	1.64(0.90–3.01)	0.103	—	
Child-pug (B vs A)	0.61(0.22–1.68)	0.341	—	
ECOG PS (1 vs 0)	0.96(0.56–1.65)	0.880	—	
Albumin (≥34.8 vs <34.8g/L)	1.20(0.73–1.98)	0.468	—	
ALT (≥38.5 vs <38.5 U/L)	1.59(0.97–2.64)	0.068	1.39(0.82–2.38)	0.225
AST (≥63.5 vs <63.5 U/L)	1.41(0.83–2.38)	0.199	—	
HBV-DNA (≥10^4 vs <10^4IU/ mL)	1.10(0.65–1.86)	0.727	—	
AFP (≥400 vs <400 ng/mL)	2.42(1.42–4.09)	0.001	2.04(1.15–3.64)	0.015
PIVKA-II (≥732 vs <732 mAU/mL)	2.25(1.33–3.81)	0.002	2.05(1.14–3.66)	0.016
NLR (≥3.2 vs <3.2)	1.45(0.88–2.39)	0.147	—	
PLR (≥136.2 vs <136.2)	1.39(0.84–2.29)	0.197	—	
Tumor numbers (≥3 vs <3个)	2.27(1.34–3.85)	0.002	2.53(1.47–4.34)	0.001
Tumor size (≥10 vs <10cm)	1.04(0.62–1.73)	0.886	—	
Tumor margin (Non-smooth vs Smooth)	1.34(0.77–2.33)	0.293	—	
Internal artery (Presence vs Absence)	1.13(0.64–2.01)	0.671	—	
Peritumoral contrast enhancement (Presence vs Absence)	1.20(0.73–1.98)	0.467	—	
Tumor in portal venous (Presence vs Absence)	1.53(0.93–2.53)	0.095	1.05(0.62–1.78)	0.860
Tumor in hepatic venous (Presence vs Absence)	1.60(0.89–2.88)	0.117		
Extrahepatic metastases (Presence vs Absence)	2.12(1.28–3.52)	0.004	1.01(0.57–1.79)	0.977
ΔAER (<15% vs ≥15%)	2.18(1.32–3.58)	0.002	2.57(1.54–4.33)	<0.001

Abbreviations: HR, hazard Ratio; ALT, alanine aminotransferase; AST, aspartate aminotransferase; AFP, alpha-fetoprotein; PIVKA-II, prothrombin induced by vitamin K absence-II; AST, aspartate aminotransferase; HBV-DNA, Hepatitis B virus DNA load; NLR, neutrophil-to-lymphocyte ratio; PLR, platelet-to-lymphocyte ratio; ΔAER, decrease ratio of arterial phase contrast-enhancement; BCLC stage, Barcelona clinic liver cancer staging system; ECOG PS, eastern cooperative oncology group performance status.

OS Predictive Model Construction and Validation

The independent factors mentioned above (NLR, tumor numbers, ΔAER, peritumoral enhancement, and extrahepatic metastasis) were used to build an OS predictive model. The model's AUC for predicting 1-year and 2-year survival rates was 0.848 (95% CI: 0.717–0.910) and 0.866 (95% CI: 0.734–0.944), respectively. Nomograms were built based on the clinical and CT features to predict the OS, calibration curves showed excellent agreement between predicted and actual probabilities, and internal validation using 1,000 bootstrap resamples yielded a C-index of 0.76, DCA further confirmed the model's clinical utility (Figure 5).

Subgroup Analysis

We performed additional subgroup analysis by cirrhosis and BCLC stage and added results to the Supplementary Materials: Subgroup Analysis.

Discussion

This study evaluated the prognostic value of combining clinical features with CT-enhanced imaging in predicting the efficacy and survival outcomes of patients with unresectable HCC treated with Camrelizumab plus Apatinib. Our results identified AFP (≥400 ng/mL), neutrophil-to-lymphocyte ratio (NLR ≥ 3.2), Tumor numbers (≥3), and arterial enhancement ratio change (ΔAER < 15%) as independent risk factors for OR, with a predictive model AUC of 0.874. Additionally, AFP (≥400 ng/mL), PIVKA-II (≥732 mAU/mL), Tumor numbers (≥3), and ΔAER (<15%) were

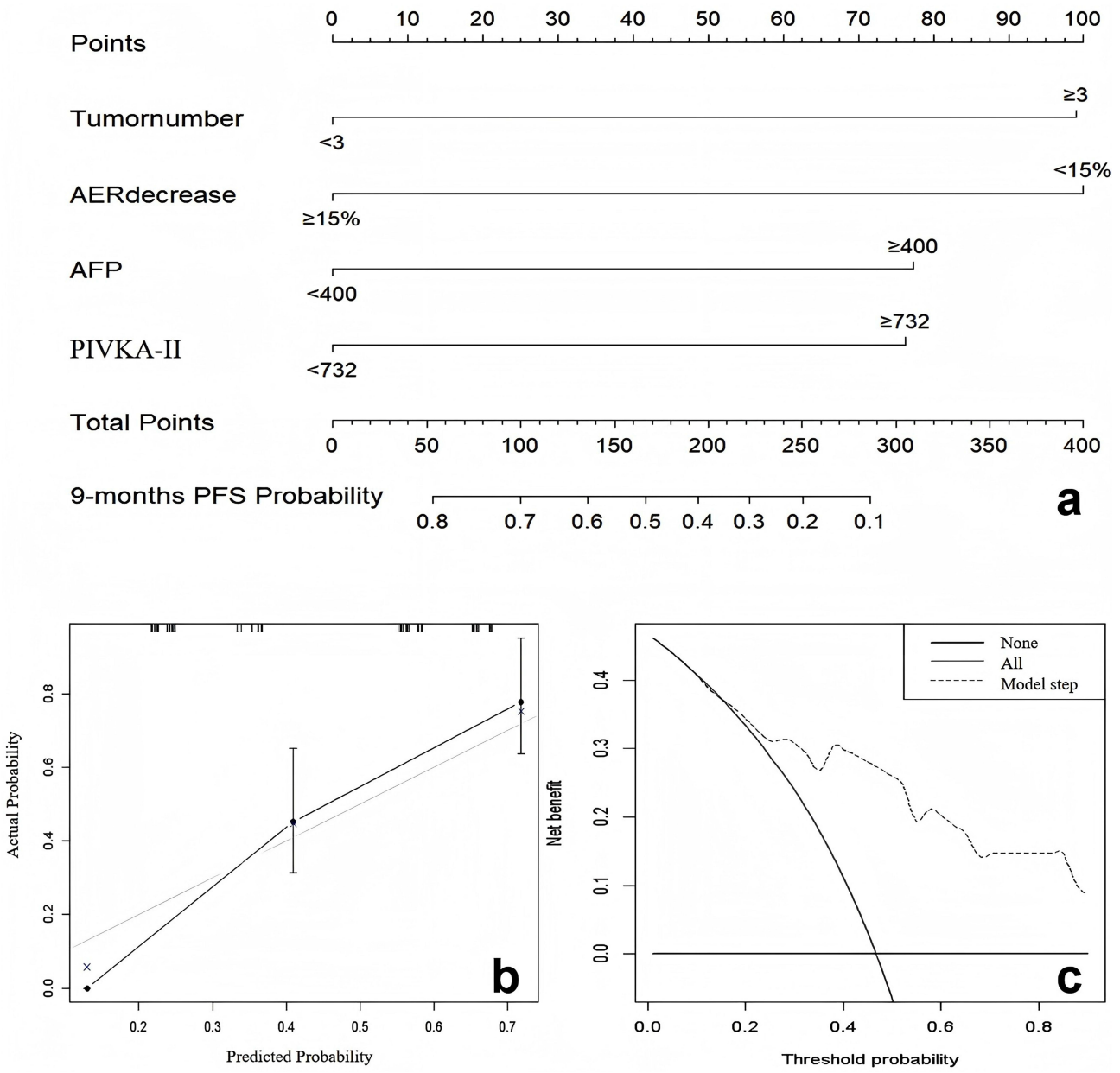

Figure 4 The nomogram to predict progression-free survival (PFS) in Camrelizumab plus Apatinib treatment for unresectable hepatocellular carcinoma. (**a**) The nomogram was developed with alpha-fetoprotein (AFP), prothrombin induced by vitamin K absence-II (PIVKA-II), tumor numbers, and a decrease ratio of arterial phase contrast-enhancement (ΔAER). A vertical line was made according to the value of the total points to determine the probability of PFS. (**b**) Validity of the predictive performance of the nomogram in estimating the risk of PFS in the 1,000 bootstrap resamples. (**c**) Decision curve analysis (DCA) of the prediction model, Y-axis represents the net benefit, the X-axis is the probability threshold.

independent predictors of PFS, with an AUC of 0.859. NLR (≥3.2), Tumor numbers (≥3), peritumoral enhancement, extrahepatic metastasis, and ΔAER (<15%) were significant predictors for OS, yielding AUCs of 0.848 and 0.866 for 1- and 2-year survival, respectively.

In this study, elevated baseline AFP (≥400 ng/mL) was an independent predictor for both ORR and PFS. This finding aligns with previous studies on HCC systemic treatment, which suggested that AFP contributes to immune escape in HCC cells, potentially through mechanisms like inducing PD-L1 expression in immune cells.[17] AFP may impair antigen presentation by inducing immunosuppressive dendritic phenotypes. Mao et al[18] demonstrated that preoperative AFP levels were strongly correlated with OS and recurrence-free survival (RFS) in HCC patients post-resection. A meta-analysis of the REACH[19] and REACH-2[20] studies also found that patients with AFP levels between 400 and 1,000 ng/mL had longer OS

Table 4 Univariate and Multivariate Cox Regression Analysis of Clinical and CT Features for Overall Survival

Variable	Univariate Cox Regression		Multivariate Cox Regression	
	HR (95% CI)	*P* value	HR (95% CI)	*P* value
Age (≥60 vs <60years)	1.10(0.56–2.16)	0.773	—	
Gender (male vs female)	0.98(0.46–2.11)	0.977	—	
Hepatitis B (Presence vs Absence)	0.90(0.32–2.50)	0.842	—	
Cirrhosis (Presence vs Absence)	1.15(0.49–2.72)	0.742	—	
BCLC stage (C vs B)	6.90(2.14–22.22)	0.001	—	
Child-pug (B vs A)	1.90(0.92–3.94)	0.082	—	
ECOG PS (1 vs 0)	1.75(0.99–3.08)	0.054	—	
Albumin (≥34.8 vs <34.8g/L)	0.73(0.41–1.28)	0.272	—	
ALT (≥38.5 vs <38.5 U/L)	1.74(0.98–3.06)	0.057	—	
AST (≥63.5 vs <63.5 U/L)	1.72(0.97–3.04)	0.062	—	
HBV-DNA (≥10^4 vs <10^4IU/ mL)	1.42(0.79–2.52)	0.236	—	
AFP (≥400 vs <400 ng/mL)	1.99(1.12–3.52)	0.018	1.36(0.74–2.53)	0.324
PIVKA-II (≥732 vs <732 mAU/mL)	1.64(0.93–2.91)	0.090	—	
NLR (≥3.2 vs <3.2)	2.45(1.38–4.34)	0.002	2.07(1.15–3.73)	0.015
PLR (≥136.2 vs <136.2)	1.23(0.70–2.17)	0.465	—	
Tumor numbers (≥3 vs <3个)	2.97(1.57–5.63)	0.001	2.68(1.38–5.21)	0.004
Tumor size (≥10 vs <10cm)	1.75(0.99–3.08)	0.053	—	
Tumor margin (Non-smooth vs Smooth)	2.85(1.33–6.10)	0.007	1.19(0.21–6.72)	0.839
Internal artery (Presence vs Absence)	1.54(0.77–3.09)	0.224	—	
Peritumoral contrast enhancement (Presence vs Absence)	1.89(1.05–3.39)	0.014	1.81(0.98–3.33)	0.049
Tumor in portal venous (Presence vs Absence)	2.03(1.14–3.62)	0.016	1.08(0.53–2.18)	0.831
Tumor in hepatic venous (Presence vs Absence)	2.32(1.25–4.03)	0.007	0.96(0.43–2.16)	0.916
Extrahepatic metastases (Presence vs Absence)	3.09(1.71–5.59)	<0.001	2.32(1.21–4.44)	0.011
ΔAER (<15% vs ≥15%)	2.14(1.22–3.77)	0.008	2.16(1.22–3.83)	0.009

Abbreviations: HR, hazard Ratio; ALT, alanine aminotransferase; AST, aspartate aminotransferase; HBV-DNA, Hepatitis B virus DNA load; AFP, alpha-fetoprotein; PIVKA-II, prothrombin induced by vitamin K absence-II; AST, aspartate aminotransferase; NLR, neutrophil-to-lymphocyte ratio; PLR, platelet-to-lymphocyte ratio; ΔAER, decrease ratio of arterial phase contrast-enhancement; BCLC stage, Barcelona clinic liver cancer staging system; ECOG PS, eastern cooperative oncology group performance status.

compared to those with AFP >1,000 ng/mL. In contrast, a study from South Korea analyzing 121 patients treated with atezolizumab plus bevacizumab reported no significant association between baseline AFP (≥400 ng/mL) and OS (p = 0.277) or PFS (p = 0.923). However, patients who showed a ≥30% decrease in AFP after treatment had a higher ORR compared to those without this decline (42.6% vs 21.5%, p = 0.017).[21] And others suggest AFP ≥400 ng/mL was independent risk factors for poor prognosisin in patients with advanced HCC after the failure of sorafenib.[22] While AFP alone may not be sufficient to predict treatment efficacy, its role as an independent risk factor for targeted immunotherapy outcomes warrants attention. This highlights regional heterogeneity in biomarker performance.

PIVKA-II is a specific tumor marker for HCC, associated with poor tumor behaviors such as proliferation, metastasis, and invasion. PIVKA-II promotes tumor thrombus formation, contributing to vascular invasion. In our study, PIVKA-II (≥732 mAU/mL) was an independent factor affecting PFS (HR = 2.05). Previous research supports PIVKA-II as a potential tool for predicting vascular invasion, metastasis, and recurrence, and it has been used to evaluate prognosis after liver resection and ablation.[23,24] Chon et al[21] also demonstrated that baseline PIVKA-II (≥186 mAU/mL) was an independent predictor of poor OS and PFS in patients treated with atezolizumab and bevacizumab, further validating its prognostic value.

In our study, baseline NLR (≥3.2) emerged as an important serum marker for predicting both OR and OS. High baseline NLR was an independent risk factor for poor treatment outcomes and shorter OS. Neutrophils produce inflammatory mediators that promote tumor development, angiogenesis, and metastasis, while lymphocytes play a role in inducing cytotoxic death and inhibiting tumor proliferation. Given that most HCC cases are linked to chronic inflammation and liver fibrosis, often caused by viral infections or other factors, NLR has been shown to affect the

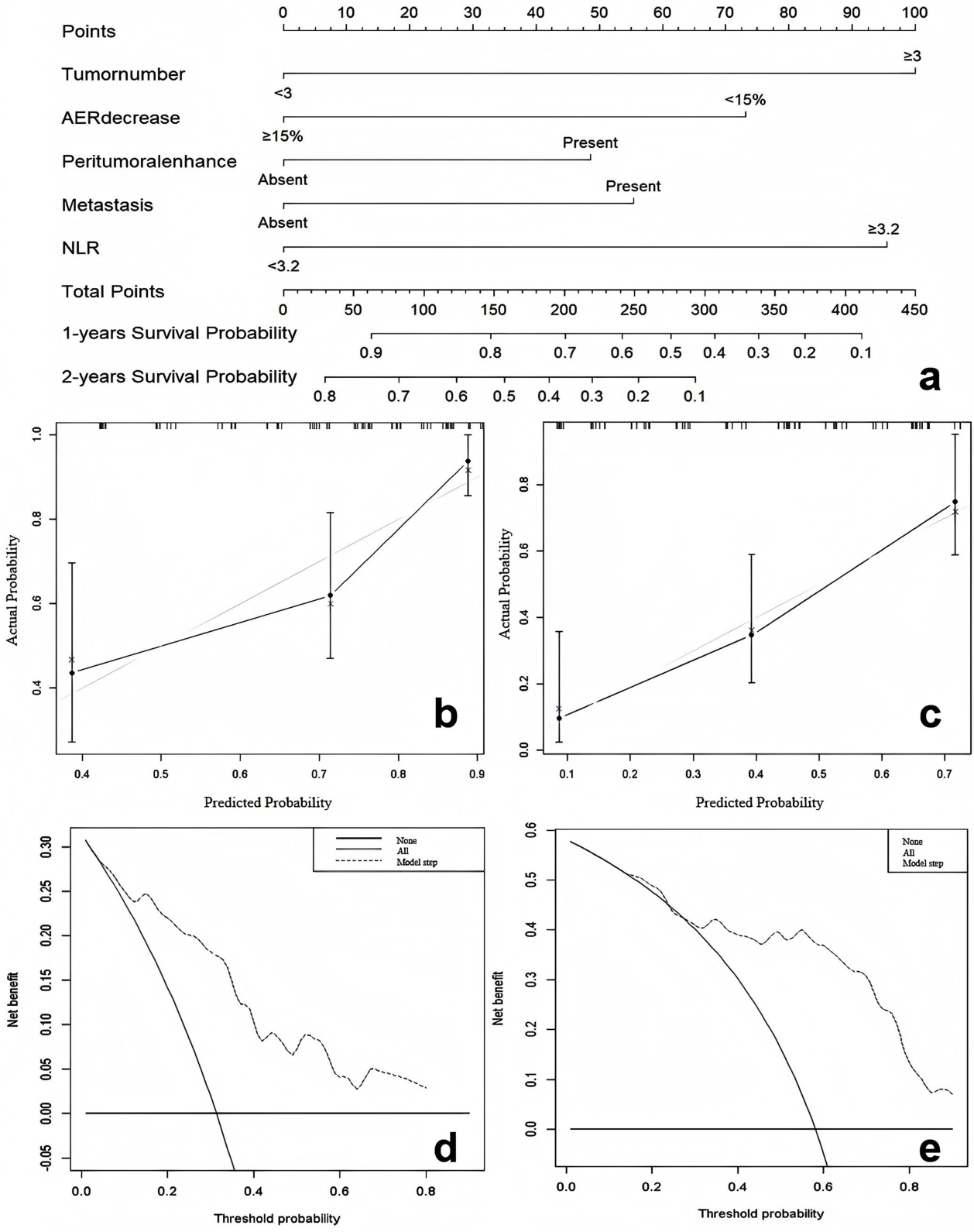

Figure 5 The nomogram to predict overall survival (OS) in Camrelizumab plus Apatinib treatment for unresectable hepatocellular carcinoma. (**a**) The nomogram was developed with neutrophil-to-lymphocyte ratio (NLR), tumor numbers, decrease ratio of arterial phase contrast-enhancement (ΔAER), peritumoral enhancement, and extrahepatic metastasis. A vertical line was made according to the value of the total points to determine the probability of OS. (**b** and **c**) Validity of the predictive performance of the nomogram in estimating the risk of OS in the 1,000 bootstrap resamples. (**d** and **e**) Decision curve analysis (DCA) of the prediction model, Y-axis represents the net benefit, the X-axis is the probability threshold.

efficacy of targeted therapy[25] or combined with immunotherapy[26] in several studies. Chon et al[27] found that patients with baseline NLR <2.5 had higher ORR than those with NLR ≥2.5 (39.0% vs 19.4%, p = 0.017). Although NLR is a simple and accessible biomarker, its optimal cut-off value remains controversial, and larger, multicenter prospective studies are needed to establish the most appropriate threshold.

Tumor numbers (≥3) was another key factor affecting both PFS and OS in our study. Existing studies reported that tumor multiplicity was an independent predictors associated with late recurrence after HCC resection,[28] and the post-operative adjuvant transarterial chemoembolization achieved significant recurrence-free survival and OS improvements in HIPC3 (internal arteries present and diameter >5 cm, or two or three tumors) patients.[29] In our study, we chose the cut-off of ≥3 tumors due to the advanced stage of our patient population, in which 69.7% had multiple tumors. A study[30] comparing TACE combined with Apatinib plus PD-1 inhibitors to TACE combined with Apatinib in advanced HCC also found that Tumor numbers ≥ 3, AFP ≥ 400 ng/mL, and distant metastasis were independent predictors of OS, consistent with our findings.

CT-enhanced imaging features were validated in our study for their prognostic value. Peritumoral contrast-enhancement was an important factor affecting OS (HR = 1.81), this feature may represent compensatory arterial hyperperfusion due to microvascular invasion,[15] which has been identified as an independent risk factor for early recurrence and poor prognosis in HCC. Additionally, ΔAER was a significant independent predictor for OR, OS, and PFS. Patients with ΔAER ≥ 15% had better ORR and improved survival. As the mechanism of action of targeted therapy primarily involves blocking tumor angiogenesis and inducing ischemic necrosis,[31] early evaluations showing reduced arterial enhancement in effective patients are expected. Colagrande et al[32] showed that the volume of enhancement of disease is a novel radiologic parameter obtained by CT arterial enhancement coefficient, which could be helpful in selecting patients who are more likely to respond to sorafenib. ΔAER is an easily obtainable and simple metric that could become a crucial indicator for evaluating the efficacy of targeted immunotherapy for HCC in the future. Although ΔAER was a strong predictor, its biological underpinning remains speculative. Further studies correlating imaging with microvessel density or necrosis are warranted.

This study has several limitations. First, its retrospective design introduces inherent selection bias, and the relatively short follow-up period prevents long-term survival analysis beyond three years. Second, being a single-center study with a limited sample size, our findings may lack generalizability, despite internal validation through 1,000 bootstrap resamples. External validation from other institutions or larger datasets is necessary to strengthen the model's applicability. Last but not least, our predictive model lacks functional MR imaging data, which could improve accuracy. Future studies incorporating radiomics and deep learning in conjunction with MRI may help build a more comprehensive prediction model.

In conclusion, our findings suggest that contrast-enhanced CT features and clinical biomarkers such as AFP, NLR, tumor multiplicity, and ΔAER are statistically associated with prognosis in unresectable HCC treated with Camrelizumab plus Apatinib. These predictors, integrated into nomograms, may aid personalized treatment planning. Future work integrating MRI radiomics and liquid biopsy maybe potentially enhance predictive accuracy and clinical translation.

Data Sharing Statement

Data used is available from the corresponding author upon reasonable request.

Ethical Approval

The studies involving human participants were reviewed and approved (Approved No. 2023-K012-01) by the Ethics Committee of First Affiliated Hospital of Guangxi Medical University (Nanning, China), and in accordance with the World Medical Association Declaration of Helsinki, the written informed consent was waived by our institutional review board.

Author Contributions

All authors made a significant contribution to the work reported, whether in the conception, study design, execution, acquisition of data, analysis and interpretation, or in all these areas; took part in drafting, revising or critically reviewing

the article; gave final approval of the version to be published; have agreed on the journal to which the article has been submitted; and agree to be accountable for all aspects of the work.

Funding

This work was funded by the National Natural Science Foundation of China (Grant No. 82060310, 82560338), the Science and Technology Department of Guangxi (Grant No. 2025GXNSFAA069531). Development Project of Hainan Provincial Clinical Medical Center, the Science and Technology Department of Hainan Province (Grant number ZDYF2024SHFZ052, 821RC677).

Disclosure

All authors declare no conflicts of interest in this work.

References

1. Bray F, Laversanne M, Sung H, et al. Global cancer statistics 2022: GLOBOCAN estimates of incidence and mortality worldwide for 36 cancers in 185 countries. *CA*. 2024;74(3):229–263. doi:10.3322/caac.21834
2. Qi J, Li M, Wang L, et al. National and subnational trends in cancer burden in China, 2005-20: an analysis of national mortality surveillance data. *Lancet Public Health*. 2023;8(12):e943–e955. doi:10.1016/s2468-2667(23)00211-6
3. Singal AG, Llovet JM, Yarchoan M, et al. AASLD practice guidance on prevention, diagnosis, and treatment of hepatocellular carcinoma. *Hepatology*. 2023;78(6):1922–1965. doi:10.1097/hep.0000000000000466
4. Yang X, Yang C, Zhang S, et al. Precision treatment in advanced hepatocellular carcinoma. *Cancer Cell*. 2024;42(2):180–197. doi:10.1016/j.ccell.2024.01.007
5. Llovet JM, Castet F, Heikenwalder M, et al. Immunotherapies for hepatocellular carcinoma. *Nat Rev Clin Oncol*. 2022;19(3):151–172. doi:10.1038/s41571-021-00573-2
6. Qin S, Chan SL, Gu S, et al. Camrelizumab plus rivoceranib versus sorafenib as first-line therapy for unresectable hepatocellular carcinoma (CARES-310): a randomised, open-label, international Phase 3 study. *Lancet*. 2023;402(10408):1133–1146. doi:10.1016/s0140-6736(23)00961-3
7. Llovet JM, Pinyol R, Kelley RK, et al. Molecular pathogenesis and systemic therapies for hepatocellular carcinoma. *Nat Cancer*. 2022;3(4):386–401. doi:10.1038/s43018-022-00357-2
8. Cheng AL, Hsu C, Chan SL, Choo SP, Kudo M. Challenges of combination therapy with immune checkpoint inhibitors for hepatocellular carcinoma. *J Hepatol*. 2020;72(2):307–319. doi:10.1016/j.jhep.2019.09.025
9. Wang Y, Zhou S, Yang F, et al. Treatment-related adverse events of PD-1 and PD-L1 inhibitors in clinical trials: a systematic review and meta-analysis. *JAMA Oncol*. 2019;5(7):1008–1019. doi:10.1001/jamaoncol.2019.0393
10. Zhang Z, Yu G, Eresen A, Hou Q, Yaghmai V, Zhang Z. MRI monitoring of combined therapy with transcatheter arterial delivery of NK cells and systemic administration of sorafenib for the treatment of HCC. *Am J Cancer Res*. 2024;14(5):2216–2227. doi:10.62347/iaro1564
11. Zhang N, Yang X, Piao M, et al. Biomarkers and prognostic factors of PD-1/PD-L1 inhibitor-based therapy in patients with advanced hepatocellular carcinoma. *Biomark Res*. 2024;12(1):26. doi:10.1186/s40364-023-00535-z
12. Bao Y, Li JX, Zhou P, et al. Identifying proliferative hepatocellular carcinoma at pretreatment CT: implications for therapeutic outcomes after transarterial chemoembolization. *Radiology*. 2023;308(2):e230457. doi:10.1148/radiol.230457
13. Gordan JD, Kennedy EB, Abou-Alfa GK, et al. Systemic therapy for advanced hepatocellular carcinoma: ASCO guideline update. *J Clin Oncol*. 2024;42(15):1830–1850. doi:10.1200/jco.23.02745
14. Zhang TQ, Geng ZJ, Zuo MX, et al. Camrelizumab (a PD-1 inhibitor) plus apatinib (an VEGFR-2 inhibitor) and hepatic artery infusion chemotherapy for hepatocellular carcinoma in barcelona clinic liver cancer stage C (TRIPLET): a Phase II study. *Signal Transduct Target Ther*. 2023;8(1):413. doi:10.1038/s41392-023-01663-6
15. Yang L, Gu D, Wei J, et al. A radiomics nomogram for preoperative prediction of microvascular invasion in hepatocellular carcinoma. *Liver Cancer*. 2019;8(5):373–386. doi:10.1159/000494099
16. Colagrande S, Calistri L, Campani C, et al. CT volume of enhancement of disease (VED) can predict the early response to treatment and overall survival in patients with advanced HCC treated with sorafenib. *Eur Radiol*. 2021;31(3):1608–1619. doi:10.1007/s00330-020-07171-3
17. Zheng Y, Zhu M, Li M. Effects of alpha-fetoprotein on the occurrence and progression of hepatocellular carcinoma. *J Cancer Res Clin Oncol*. 2020;146(10):2439–2446. doi:10.1007/s00432-020-03331-6
18. Mao S, Yu X, Sun J, et al. Development of nomogram models of inflammatory markers based on clinical database to predict prognosis for hepatocellular carcinoma after surgical resection. *BMC Cancer*. 2022;22(1):249. doi:10.1186/s12885-022-09345-2
19. Zhu AX, Park JO, Ryoo BY, et al. Ramucirumab versus placebo as second-line treatment in patients with advanced hepatocellular carcinoma following first-line therapy with sorafenib (REACH): a randomised, double-blind, multicentre, phase 3 trial. *Lancet Oncol*. 2015;16(7):859–870. doi:10.1016/s1470-2045(15)00050-9
20. Zhu AX, Kang YK, Yen CJ, et al. Ramucirumab after sorafenib in patients with advanced hepatocellular carcinoma and increased α-fetoprotein concentrations (REACH-2): a randomised, double-blind, placebo-controlled, phase 3 trial. *Lancet Oncol*. 2019;20(2):282–296. doi:10.1016/s1470-2045(18)30937-9
21. Chon YE, Cheon J, Kim H, et al. Predictive biomarkers of survival in patients with advanced hepatocellular carcinoma receiving atezolizumab plus bevacizumab treatment. *Cancer Med*. 2023;12(3):2731–2738. doi:10.1002/cam4.5161
22. Xu Y, Fu S, Liu K, Mao Y, Wu J. Lenvatinib Plus PD-1 Inhibitors versus regorafenib in patients with advanced hepatocellular carcinoma after the failure of sorafenib: a retrospective study. *Ther Clin Risk Manag*. 2023;19:853–863. doi:10.2147/tcrm.S420371

23. Masuda T, Beppu T, Okabe H, et al. Predictive factors of pathological vascular invasion in hepatocellular carcinoma within 3 cm and three nodules without radiological vascular invasion. *Hepatol Res*. 2016;46(10):985–991. doi:10.1111/hepr.12637
24. Zhang D, Liu Z, Yin X, et al. Prognostic value of PIVKA-II in hepatocellular carcinoma patients receiving curative ablation: a systematic review and meta-analysis. *Int J Biol Markers*. 2018;33(3):266–274. doi:10.1177/1724600818760234
25. Tada T, Kumada T, Hiraoka A, et al. Neutrophil-to-lymphocyte ratio is associated with survival in patients with unresectable hepatocellular carcinoma treated with lenvatinib. *Liver Int*. 2020;40(4):968–976. doi:10.1111/liv.14405
26. Xiao Y, Zhu G, Xie J, et al. Pretreatment neutrophil-to-lymphocyte ratio as prognostic biomarkers in patients with unresectable hepatocellular carcinoma treated with hepatic arterial infusion chemotherapy combined with lenvatinib and camrelizumab. *J Hepatocell Carcinoma*. 2023;10:2049–2058. doi:10.2147/jhc.S432134
27. Chon YE, Park H, Hyun HK, et al. Development of a new nomogram including neutrophil-to-lymphocyte ratio to predict survival in patients with hepatocellular carcinoma undergoing transarterial chemoembolization. *Cancers*. 2019;11(4). doi:10.3390/cancers11040509
28. Yan WT, Li C, Yao LQ, et al. Predictors and long-term prognosis of early and late recurrence for patients undergoing hepatic resection of hepatocellular carcinoma: a large-scale multicenter study. *Hepatobiliary Surg Nutr*. 2023;12(2):155–168. doi:10.21037/hbsn-21-288
29. Li X, Liang X, Li Z, et al. A novel stratification scheme combined with internal arteries in CT imaging for guiding postoperative adjuvant transarterial chemoembolization in hepatocellular carcinoma: a retrospective cohort study. *Int J Surg*. 2024;110(5):2556–2567. doi:10.1097/js9.0000000000001191
30. Xia WL, Zhao XH, Guo Y, et al. Transarterial chemoembolization combined with apatinib with or without PD-1 inhibitors in BCLC stage C hepatocellular carcinoma: a multicenter retrospective study. *Front Oncol*. 2022;12:961394. doi:10.3389/fonc.2022.961394
31. Zhu XD, Tang ZY, Sun HC. Targeting angiogenesis for liver cancer: past, present, and future. *Genes Dis*. 2020;7(3):328–335. doi:10.1016/j.gendis.2020.03.010
32. Colagrande S, Calistri L, Campani C, et al. Correction to: CT volume of enhancement of disease (VED) can predict the early response to treatment and overall survival in patients with advanced HCC treated with sorafenib. *Eur Radiol*. 2021;31(6):4409. doi:10.1007/s00330-020-07592-0